J. Plasma Physics (2014), *vol.* 80, *part* 3, *pp.* 379–393. © Cambridge University Press 2013
doi:10.1017/S0022377813001347

Dispersion equation for ballooning modes in two-component plasma

D. A. Kozlov[1], N. G. Mazur[2], V. A. Pilipenko[3],† and E. N. Fedorov[2]

[1]Institute of Solar-Terrestrial Physics, Irkutsk, Russia
[2]Institute of Physics of the Earth, 123995 Moscow, Russia
[3]Space Research Institute, 117997 Moscow, Russia

(Received 30 May 2013; revised 30 September 2013; accepted 15 October 2013;
first published online 13 December 2013)

The ballooning magnetohydrodynamic (MHD) modes have been often suggested as a possible instability trigger of the substorm onset, and a mechanism of compressional waves in the outer magnetosphere and magnetotail. Commonly, these disturbances are characterized by the local dispersion equation that is widely applied for the description of ultra-low-frequency oscillatory disturbances and instabilities in the nightside magnetosphere. In realistic situations, especially in the inner magnetosphere, the magnetospheric plasma is composed of two components: background 'cold' plasma and 'hot' particles. The ballooning disturbances in a two-component plasma immersed into a curved magnetic field are described with the system of coupled equations for the Alfvén and slow magnetosonic (SMS) modes. We have reduced the basic system of MHD equations to the dispersion equation for the small-scale in transverse direction disturbances, and applied WKB approximation along a field line. As a result, we have derived a dispersion equation that can be used for geophysical applications. In particular, from this relationship the dispersion, instability threshold, and stop-bands of the Alfvén and SMS modes in two-component plasma have been examined.

1. Introduction: Ballooning modes in the near-Earth plasma

The ballooning instability could be a possible trigger of the substorm explosive phase as was suggested by Miura et al. (1989) and Ohtani and Tamao (1993). Later, this idea was extensively elaborated (Cheng and Qian 1994; Liu 1997; Agapitov et al. 2007). Favorable conditions for the growth of this instability emerge at a steep plasma pressure drop held by curved field lines. Such a condition may occur before substorm onset on strongly extended field lines (Zhu et al. 2009). Though the main substorm power is released via reconnection in the distant magnetotail, the substorm onset trigger could be the ballooning instability in a region of closed field lines (Raeder et al. 2010). There are other magnetospheric regions where the ballooning instability may develop: outer boundary of the trapped radiation (Pokhotelov et al. 1980), at the westward traveling surge (Roux et al. 1991). This instability can be imagined as a localized disruption of plasma pressure gradient by growing small-scale 'fingers' of hot plasma. To better understand the physical mechanisms of the processes involved in the substorm development, the results of the numerical modeling and *in situ*

† Email address for correspondence: pilipenk@augsburg.edu

https://doi.org/10.1017/S0022377813001347 Published online by Cambridge University Press

satellite observations are to be compared with simplified, but more explicit, theoretical models.

Ultra-Low-Frequency (ULF) waves of the Pc5 frequency range (periods about 3–10 min) – so called storm-time Pc5 pulsations – are a ubiquitous element of magnetic storms. These long-lasting (from several hours to tens of hours) monochromatic oscillations are supposedly generated by ring current protons during the magnetic storm recovery phase. A feature of these pulsations is a significant field-aligned (compressional) magnetic component and small azimuthal scale (wave numbers $m \simeq 30 - 100$). Many theories (e.g. Southwood and Saunders 1985; Cheremnykh and Parnowski 2004) were aimed to understand the physics of compressional Pc5 waves persistently observed by space-borne magnetometers. Various kinds of kinetic instabilities of ring current ions were suggested as a possible excitation mechanism of these waves (Pokhotelov et al. 1985; Cheng and Lin 1987; Cheng et al. 1994).

ULF waves also play an active role in the dynamics (energy transport, dissipation, and sink) of the Earth's magnetotail (Keiling 2009). Geotail satellite observations in the magnetotail from 9 to 30 R_E indicated coupling of slow mode and transverse Alfvén wave (Nakamizo and Iijima 2003). The mode conversion between the Alfvén and slow mode waves were observed by the THEMIS spacecraft constellation in the region of the central current sheet (Du et al. 2011). Thus, coupled magnetohydrodynamic (MHD) modes are a vital component of dynamic magnetotail and outer magnetosphere. The ballooning MHD instability was suggested to be a trigger for the destabilization of the solar coronal loops and flare energy release (Tsap et al. 2008).

A theoretical approach to the study of the ballooning modes and their stability is based on a complicated system of coupled equations for the poloidal Alfvén waves and slow magnetosonic (SMS) modes in a finite-pressure plasma immersed in a curved magnetic field $\boldsymbol{B}$. The easiest way to comprehend qualitatively the basic features of the unstable modes and instability condition is the analysis of a local dispersion equation. Such a dispersion equation, obtained using a local analysis of this system, is widely used for geophysical applications both for examination of plasma stability (Liu 1997), and for the description of spectral properties of ULF wave phenomena in the nightside auroral magnetosphere (Safargaleev and Maltsev 1986; Golovchanskaya and Maltsev 2005; Golovchanskaya and Mingalev 2006). The most detailed and comprehensive derivation and analysis of the dispersion equation was provided by Mazur et al. (2012).

However, in all the above papers it was assumed that plasma had one component with a finite temperature. In realistic situations, especially in the outer magnetosphere, the magnetospheric plasma is composed of two components (Walker 1987):

— background 'cold' plasma with density ρ_{c0}, and

— 'hot' component with density ρ_{h0} that is responsible for a finite plasma pressure.

The two-component plasma may be characterized, e.g. by the fraction of the hot component $\mu = \rho_{h0}/(\rho_{c0} + \rho_{h0})$ (for one-component plasma $\mu = 1$).

Moreover, the previous studies considered two-dimensional (2D) geometry, where the coordinate lines were straight in Y (azimuthal) direction. In reality, the magnetospheric system is torus-like; therefore, the magnetic shell curvature in the azimuthal direction may influence the wave properties. In this paper, we derive and analyze the dispersion equation with the account of these aspects: two-component plasma and curved magnetic shells in the azimuthal direction.

https://doi.org/10.1017/S0022377813001347 Published online by Cambridge University Press

2. MHD plasma equilibrium and linearized dynamic equations

2.1. *Basic equations*

We consider the plasma consisting of cold and hot ions in a curvilinear magnetic field. The set of MHD equations in this case is (Walker 1987):

$$\rho_h \frac{d\boldsymbol{V}_h}{dt} = -\nabla P + c^{-1}\boldsymbol{J}_h \times \boldsymbol{B}, \tag{2.1}$$

$$\frac{\partial \rho_h}{\partial t} + \nabla \rho_h \boldsymbol{V}_h = 0, \tag{2.2}$$

$$\rho_c \frac{d\boldsymbol{V}_c}{dt} = c^{-1}\boldsymbol{J}_c \times \boldsymbol{B}, \tag{2.3}$$

$$\frac{\partial \rho_c}{\partial t} + \nabla \rho_c \boldsymbol{V}_c = 0, \tag{2.4}$$

$$\frac{d}{dt}\left(\frac{P}{\rho_h^{\gamma}}\right) = 0, \tag{2.5}$$

$$\nabla \times \boldsymbol{E} = -c^{-1}\frac{\partial \boldsymbol{B}}{\partial t}, \qquad \nabla \times \boldsymbol{B} = 4\pi c^{-1}(\boldsymbol{J}_h + \boldsymbol{J}_c), \tag{2.6}$$

$$\boldsymbol{E} = -c^{-1}\boldsymbol{V}_c \times \boldsymbol{B} = -c^{-1}\boldsymbol{V}_h \times \boldsymbol{B}, \tag{2.7}$$

where $\boldsymbol{V}_{c,h}$ and $\rho_{c,h}$ are the velocities and densities of cold and hot plasma components, P is the plasma pressure, $\boldsymbol{B}$ is the magnetic field, $\boldsymbol{J}_{c,h}$ is the current density transported by cold and hot particles, $\boldsymbol{E}$ is the electric field, γ is the adiabatic index, and $d/dt = \partial/\partial t + (\boldsymbol{V}\nabla)$ is the Lagrangian derivative. Thus, it was supposed that in MHD limit both cold and hot particles oscillate in a wave electric field with the same transverse velocity, implying the frozen-in condition (Walker 1987).

We introduce the right-handed orthogonal curvilinear coordinates associated with the background axisymmetric magnetic field geometry $\boldsymbol{B}_0$: the x^3 coordinate is directed along the background magnetic field; therefore, $\boldsymbol{B}_0 = (0, 0, B_0)$, where B_0 is the scaled component of $\boldsymbol{B}_0$, the x^1 coordinate is across magnetic shells, and the x^2 coordinate is in the azimuthal direction.

Assuming that plasma is immobile in the stationary state, $\boldsymbol{V}_{0c} = \boldsymbol{V}_{0h} = 0$, we get the local equilibrium condition:

$$\nabla_1 P_0 + \frac{1}{4\pi} h_3^{-1} B_0 \nabla_1 h_3 B_0 = 0, \tag{2.8}$$

where $\nabla_i \equiv h_i^{-1}\partial/\partial x^i$, $h_i = \sqrt{g_i}$ are scale factors, and $g_i \equiv g_{ii}$ are diagonal components of the metric tensor. The condition (2.8) can be written in terms of κ-parameters:

$$(\beta/2)\kappa_P + \kappa_B - \kappa_c = 0,$$

where $\kappa_P = \nabla_1 \ln P_0$, $\kappa_B = \nabla_1 \ln B_0$, $\kappa_c = -\nabla_1 \ln h_3$ is the curvature of magnetic field line, $\beta = 8\pi P_0/B_0^2$. The pressure P_0 is constant along the field line, $\nabla_3 P_0 = 0$. Due to axial symmetry of the medium, all the unperturbed parameters are uniform in the azimuthal direction.

We introduce the displacement vectors $\boldsymbol{\xi}_{c,h}$ and linearize the set of equations (2.1)–(2.7) with respect to the small monochromatic perturbation $\sim \exp(-i\omega t + ik_2 h_2 x^2)$ as

https://doi.org/10.1017/S0022377813001347 Published online by Cambridge University Press

follows:

$$p = -\boldsymbol{\xi_h}\nabla P_0 - \gamma P_0 \nabla \boldsymbol{\xi}_h, \tag{2.9}$$

$$\boldsymbol{E} = i\omega c^{-1}\boldsymbol{\xi}_{c(h)} \times \boldsymbol{B}_0, \tag{2.10}$$

$$\nabla \times \boldsymbol{E} = i\omega c^{-1}\boldsymbol{b}, \tag{2.11}$$

$$-\omega^2(\rho_{h0}\boldsymbol{\xi}_h + \rho_{c0}\boldsymbol{\xi}_c) = -\nabla p - 4\pi^{-1}\boldsymbol{b} \times [\nabla \times \boldsymbol{B}_0] - 4\pi^{-1}\boldsymbol{B}_0 \times [\nabla \times \boldsymbol{b}]. \tag{2.12}$$

The linearized equation (2.4) is not included in this system because the cold plasma density perturbation $\delta\rho_c$ is only in this equation, and it may be found *a posteriori*. On the contrary, the perturbation $\delta\rho_h$ is present in the two linearized equations (2.2) and (2.5), and excluding $\delta\rho_h$ from those equations we get the relationship (2.9).

Noticing that $\xi_{c1} = \xi_{h1}$, $\xi_{c2} = \xi_{h2}$ from linearized (2.7), and $\xi_{c3} = 0$ from linearized (2.3), we denote $\xi_1 = \xi_{h1}$, $\xi_2 = \xi_{h2}$, $\xi_3 = \xi_{h3}$. Excluding the perturbed electric field $\boldsymbol{E}$ from (2.11), we obtain a closed set of equations for $\boldsymbol{b}$, $\boldsymbol{\xi}$, and p:

$$p = -\xi_1 \nabla_1 P_0 - \gamma P_0 u, \tag{2.13}$$

$$b_1 = h_2^{-1}\nabla_3 h_2 B_0 \xi_1, \tag{2.14}$$

$$b_2 = h_1^{-1}\nabla_3 h_1 B_0 \xi_2, \tag{2.15}$$

$$b_3 = -h_2^{-1}\nabla_1 h_2 B_0 \xi_1 - i B_0 k_2 \xi_2, \tag{2.16}$$

$$\omega^2\rho_0\xi_1 = \nabla_1 p + (4\pi h_3)^{-1} b_3 \nabla_1 h_3 B_0 + (4\pi h_3)^{-1} B_0 \nabla_1 h_3 b_3 - (4\pi h_1)^{-1} B_0 \nabla_3 h_1 b_1, \tag{2.17}$$

$$\omega^2\rho_0\xi_2 = ik_2 p + ik_2(4\pi)^{-1} B_0 b_3 - (4\pi h_2)^{-1} B_0 \nabla_3 h_2 b_2, \tag{2.18}$$

$$\omega^2\rho_{h0}\xi_3 = \nabla_3 p - (4\pi h_3)^{-1} b_1 \nabla_1 h_3 B_0, \tag{2.19}$$

where $\rho_0 = \rho_{c0} + \rho_{h0}$, and b_i, ξ_i, k_i are scaled components of vectors $\boldsymbol{b}$, $\boldsymbol{\xi}$, $\boldsymbol{k}$ correspondingly.

The variable $u = \nabla \cdot \boldsymbol{\xi} = (h_2 h_3)^{-1}\nabla_1 h_2 h_3 \xi_1 + ik_2\xi_2 + (h_1 h_2)^{-1}\nabla_3 h_1 h_2 \xi_3$ characterizes the plasma compression. Substituting the expressions for p and b_1 from (2.13) and (2.14) into (2.19), one can find an important relationship between the field-aligned plasma displacement ξ_3 and the plasma compression u:

$$\xi_3 = -k_s^{-2}\nabla_3 u,$$

where $k_s = \omega / V_s$, and $V_s = \sqrt{\gamma P_0/\rho_{h0}}$ is the sound speed determined by hot particles.

Excluding $\boldsymbol{b}$ from (2.13)–(2.19) and proceeding from ξ_3 and p to variables u and $\bar{p}$, where $\bar{p} = 4\pi B_0^{-2}(p + B_0 b_3/4\pi)$ is the normalized perturbation of the total pressure, we obtain the following equations:

$$\begin{aligned}
&L_P \xi_1 = \nabla_1 \bar{p} - \beta\kappa_P \bar{p} - \gamma\beta\kappa_c u - \beta\kappa_c\kappa_P \xi_1,\\
&L_T \xi_2 = ik_2 \bar{p},\\
&k_s^{-2}\left(L_s + \mu k_A^2\right) u = -\bar{p} - 2\kappa_c \xi_1,\\
&k_s^{-2} L_s u = \nabla_1 \xi_1 + ik_2 \xi_2 - \kappa_c \xi_1 + (\nabla_1 \ln h_2)\xi_1.
\end{aligned} \tag{2.20}$$

Here $\mu = \rho_{h0}/\rho_0$ is the fraction of the hot component, and the following differential operators are introduced:

$$\begin{aligned}
L_P &= k_A^2 + h_2 \nabla_3 h_1 h_2^{-1} \nabla_3 h_1^{-1},\\
L_T &= k_A^2 + h_1 \nabla_3 h_2 h_1^{-1} \nabla_3 h_2^{-1},\\
L_s &= k_s^2\left(1 + (h_1 h_2)^{-1}\nabla_3 h_1 h_2 k_s^{-2}\nabla_3\right),
\end{aligned}$$

https://doi.org/10.1017/S0022377813001347 Published online by Cambridge University Press

where $k_A = \omega / V_A$ is the Alfvén wave number, $V_A = B_0/\sqrt{4\pi\rho_0}$ is the Alfvén speed. The system (2.20) for one-component plasma coincides with the system derived in Cheng (2003) for 2D case.

2.2. *Asymptotic theory of small-scale disturbances*

Ballooning disturbances are small-scale across the main magnetic field, so their transverse structure can be described in the geometric optics approximation. Namely, we search a solution of the system (2.20) in the following form ($n = 1, 2$)

$$(\xi_n, u, \bar{p}) = [(\xi_{n0}, u_0, \bar{p}_0) + \varepsilon(\xi_{n1}, u_1, \bar{p}_1) + \varepsilon^2(\xi_{n2}, u_2, \bar{p}_2) + \ldots) \exp[i\theta(x_1)\varepsilon^{-1}],$$

where the function $\theta(x_1)$ is considered to be of order 1, and small parameter ε provides a rapid variation of phase $\theta(x_1)/\varepsilon$ across field lines. We put this decomposition into the system (2.20). Collecting terms with the same order of ε, we get in the order of ε^{-1} the system

$$k_1\xi_{10} + k_2\xi_{20} = 0, \qquad k_1\bar{p}_0 = 0, \qquad k_2\bar{p}_0 = 0, \tag{2.21}$$

where $k_1 = \theta'(x_1)$. It follows from this system that the perturbation of the total pressure $\bar{p}$ is small value of the order of $\leqslant \varepsilon$, which means decoupling of a fast magnetosonic wave.

Further, in the zeroth order of ε we get the system

$$ik_1\xi_{11} - \kappa_c\xi_{10} + (\nabla_1 \ln h_2)\xi_{10} + ik_2\xi_{21} - k_s^{-2}L_s u_0 = 0, \tag{2.22}$$

$$(L_P + \beta\kappa_c\kappa_p)\xi_{10} + \gamma\beta\kappa_c u_0 + \beta\kappa_p\bar{p}_0 - ik_1\bar{p}_1 = 0, \tag{2.23}$$

$$L_T\xi_{20} - ik_2\bar{p}_1 = 0, \tag{2.24}$$

$$2\kappa_c\xi_{10} + k_s^{-2}\left(L_s + \mu k_A^2\right)u_0 + \bar{p}_0 = 0. \tag{2.25}$$

Excluding $\bar{p}_0$ and ξ_{20} from (2.23)–(2.25) with the help of (2.21) and then excluding also the variable $\bar{p}_1$, we obtain the closed system of zero approximation equations (where zero indices are omitted for brevity)

$$\begin{aligned} &\left(L_P + k_1^2k_2^{-2}L_T + \beta\kappa_c\kappa_P\right)\xi_1 + \gamma\beta\kappa_c u = 0, \\ &2\kappa_c k_s^2\xi_1 + (L_s + \mu k_A^2)u = 0. \end{aligned} \tag{2.26}$$

This system of ordinary differential equations for the coupled Alfvén and SMS modes describes the ballooning disturbances. These equations in the case of one-component plasma ($\mu = 1$) coincide with equations from Walker (1987) and Klimushkin (1998).

3. Local dispersion equation

The spectral properties of the ballooning modes can be qualitatively understood with the use of local dispersion equations. Let us suppose that a disturbance has a small scale not only in the transverse direction, but also along the field line x^3.

In the geometrical optics (WKB) approximation $\propto \exp(ik_3h_3x^3)$ all operators turn into numerical factors $L_P = L_T = k_A^2 - k_\parallel^2$, where $k_\parallel^2 \equiv k_3^2$. Then the local dispersion equation stemming from the system (2.26) has the following form:

$$\left(\omega^2 - k_\parallel^2V_A^2\right)\left(\omega^2 - k_\parallel^2V_{ms}^2\right) + \sin^2\theta\left[\beta\kappa_c\kappa_P V_A^2\left(\omega^2 - k_\parallel^2V_{ms}^2\right) - 4\omega^2\mu\kappa_c^2V_{ms}^2\right] = 0, \tag{3.1}$$

where $\sin^2\theta = k_2^2/(k_1^2 + k_2^2)$, and $V_{ms}^2 = V_A^2V_s^2/(V_A^2 + \mu V_s^2)$ is the characteristic magnetosonic speed.

The important distinction from the case of one-component plasma ($\mu = 1$) is that in a two-component plasma the magnetosonic speed V_{ms} may exceed the Alfvén speed

https://doi.org/10.1017/S0022377813001347 Published online by Cambridge University Press

V_A. This possibility emerges under $V_s > V_A$ when μ is sufficiently small, namely

$$\mu < 1 - V_A^2/V_s^2. \tag{3.2}$$

If $V_s \leqslant V_A$, then under any μ the magnetosonic speed is still less than the Alfvén speed, $V_{ms} < V_A$. The condition (3.2) can be used during consideration of plasma with fixed temperature of hot component. However, if the parameter β is considered to be fixed, the condition (3.2) should be replaced by $\mu < \gamma\beta(2+\gamma\beta)^{-1}$.

In the cold limit ($\beta \to 0$), (3.1) reduces to the Alfvén dispersion equation in a cold plasma: $\omega^2 - k_\parallel^2 V_{Ac}^2 = 0$, where $V_{Ac} = B_0/\sqrt{4\pi\rho_{0c}}$. When the hot component predominates over cold ion population, $\mu \to 1$, then (3.1) transforms to the dispersion equation for one-component plasma with finite pressure. The obtained local dispersion equation for the axial symmetric case coincides with the equation for 2D case with straight Y-axis.

Equation (3.1) is a quadratic equation in respect to ω^2. The roots ω^2 of (3.1) are real for a real $k_\parallel$

$$\omega_\pm^2 = \frac{V_A^2}{2+\gamma\beta}\left[\sigma k_\parallel^2 + H \pm \sqrt{\left(\tau k_\parallel^2 + H\right)^2 + 4\mu^{-1}\gamma^2\beta^2\kappa_c^2 k_\parallel^2 \sin^2\theta}\right], \tag{3.3}$$

where $H = \beta\kappa_c\left[2\gamma\kappa_c - \kappa_p(2+\gamma\beta)/2\right]\sin^2\theta$, $\sigma = 1 + \gamma\beta(\mu^{-1}+1)/2$, and $\tau = 1 - \gamma\beta(\mu^{-1}-1)/2$. The relationship (3.3) describes two branches: fast (ω_+), which transforms into an Alfvén wave as $\beta \to 0$, and slow (ω_-) branch.

The fast branch $\omega_+^2(k_\parallel) > 0$ is stable for any real $k_\parallel$. Only the slow mode $\omega_-^2(k_\parallel)$ can be unstable under the condition

$$\beta\kappa_c\kappa_P \sin^2\theta > k_\parallel^2. \tag{3.4}$$

This inequality is the generalization of the ballooning instability condition for oblique disturbance $k_1 \neq 0$ (Liu 1997) and has the same form as the instability condition for the slow mode in one-component plasma.

The asymptotic formulas for disturbances with small scales in the field-aligned direction are obtained from (3.3) under assumption $k_\parallel \gg \kappa_c \sin\theta$. They depend on the sign of the coefficient τ in (3.3). When $\mu > \gamma\beta/(2+\gamma\beta)$ this value is positive, and the asymptotic formulas have the form

$$\omega_+^2 = L_A(k_\parallel^2) + O(k_\parallel^{-2}), \quad \omega_-^2 = L_{ms}(k_\parallel^2) + O(k_\parallel^{-2}),$$

where

$$L_A(k_\parallel^2) = V_A^2 k_\parallel^2 + V_A^2\kappa_c^2\beta\left[2\gamma\left(1 + \frac{(1-\mu)\gamma\beta}{\mu(2+\gamma\beta) - \gamma\beta}\right) - \frac{\kappa_P}{\kappa_c}\right]\sin^2\theta \tag{3.5}$$

and

$$L_{ms}(k_\parallel^2) = V_{ms}^2 k_\parallel^2 - \frac{4V_{ms}^2\kappa_c^2\gamma\beta\mu\sin^2\theta}{\mu(2+\gamma\beta) - \gamma\beta}. \tag{3.6}$$

Otherwise, if $\mu < \gamma\beta/(2+\gamma\beta)$, then the characteristic speed V_{ms} exceeds V_A, and the asymptotics changes to

$$\omega_+^2 = L_{ms}(k_\parallel^2) + O(k_\parallel^{-2}), \qquad \omega_-^2 = L_A(k_\parallel^2) + O(k_\parallel^{-2}).$$

The oscillation branches may be classified according to their asymptotics in the limit $k_\parallel \to \infty$. The branch with asymptotics $\omega^2 \approx L_A(k_\parallel^2)$ may be called Alfvén branch, whereas the branch with asymptotics $\omega^2 \approx L_{ms}(k_\parallel^2)$ may be called magnetosonic one.

https://doi.org/10.1017/S0022377813001347 Published online by Cambridge University Press

It is worth noting that in a two-component plasma the magnetosonic branch can become a fast branch, which can never happen in a one-component plasma. For that it is necessary the hot component temperature to be rather high, $V_s > V_A$, and the fraction of hot component density to be sufficiently small (see (3.2)).

Alfvén and magnetosonic branches are distinguished not by their speeds only, but by their polarizations as well. Short-wavelength Alfvén waves ($k_\parallel \to \infty$) are transverse, whereas magnetosonic waves are compressional (see (3.9) and (3.10)). However, under finite wave number $k_\parallel$, owing to the mode coupling described by the ballooning system (2.26), this distinction does not hold, and two branches have both transverse and compressional components.

The wave magnetic components can be derived via the variables ξ_1 and u from the system (2.26) as follows:

$$b_3 = B_0(\beta/2)(\kappa_P \xi_1 + \gamma u), \qquad b_1 = h_2^{-1}\nabla_3(h_2 B_0 \xi_1).$$

From these relationships, and using in the WKB limit $b_1 = ik_\parallel B_0 \xi_1$, the ratio between the field-aligned and transverse magnetic components can be derived via the ratio u/ξ_1:

$$b_3/b_1 = \beta(2ik_\parallel)^{-1}(\kappa_P + \gamma u/\xi_1). \tag{3.7}$$

For poloidal oscillations, that is if $k_1 \ll k_2$, from the WKB limit of the system (2.26) with account for the dispersion equation (3.1) the ratio u/ξ_1 can be found explicitly. Using it in (3.7), we obtain the dependence of the ratio between the compressional and transverse magnetic components on wave number and plasma parameters

$$\frac{b_3}{b_1} = \frac{k_\parallel}{2i\kappa_c}\left(1 - \frac{\omega_\pm^2}{k_\parallel^2 V_A^2}\right), \tag{3.8}$$

where $\omega_\pm^2$ is one of the dispersion equation branches (3.3). At $k_\parallel \to \infty$ in accordance with asymptotic formulas (3.5) and (3.6), the ratio b_3/b_1 for Alfvénic branch is as follows,

$$\frac{b_3}{b_1} \approx \frac{i\beta\kappa_c}{2k_\parallel}\left[2\gamma - \frac{\kappa_P}{\kappa_c} + \frac{2(1-\mu)\gamma^2\beta}{\mu(2+\gamma\beta) - \gamma\beta}\right], \tag{3.9}$$

whereas for the magnetosonic branch this ratio is

$$\frac{b_3}{b_1} \approx \frac{k_\parallel}{2i\kappa_c}\left(1 - \frac{\gamma\beta}{\mu(2+\gamma\beta)}\right). \tag{3.10}$$

The analysis of the formula (3.8) shows that in a stable, nearly one-component hot plasma at $\mu > \mu_\beta^* = \gamma\beta/(2+\gamma\beta)$, the wave polarization corresponds to the mode classification in the short wavelength limit; however, at smaller $k_\parallel$ it changes to the opposite. At the same time, when hot plasma component is small ($\mu < \mu_\beta^*$) because of the asymptotics swapping at $\mu = \mu_\beta^*$, the Alfvénic branch polarization is predominantly transverse at all $k_\parallel$. The same is valid for magnetosonic branch: at small μ its polarization is predominantly compressional at all $k_\parallel$. In a potentially unstable plasma with $\kappa_P/\kappa_c > 0$, the growing slow mode under condition (3.4) has a magnitude of the ratio $b_3/b_1 \gtrsim 1/2$.

3.1. *The possibility of total reflection of the poloidal Alfvén waves*

Analysis of the dispersion equation (3.3) shows that for the real ω there may occur regions where $k_\parallel^2 < 0$. These regions with high β and locally curved field lines are non-transparent for poloidal Alfvén waves (Mager et al. 2009). A wave meets the

https://doi.org/10.1017/S0022377813001347 Published online by Cambridge University Press

turning points $k_\parallel^2 = 0$ when its frequency ω matches the cut-off frequency

$$\omega_*^2 = \omega_+^2(0) = \beta V_A^2 \kappa_c^2 \left(\frac{4\gamma}{2+\gamma\beta} - \frac{\kappa_P}{\kappa_c} \right) \sin^2\theta = \frac{2P_0}{\rho_0} \kappa_c^2 \left(\frac{4\gamma}{2+\gamma\beta} - \frac{\kappa_P}{\kappa_c} \right) \sin^2\theta. \quad (3.11)$$

When $\kappa_P/\kappa_c \ll 1$, the cut-off frequency distribution along a field line can be estimated as $\omega_*^2 \sim 1/(R_c^2\rho_0)$ because P_0 is constant along the field line. Both the curvature radius R_c of the field line and the plasma density $\rho_0 = \rho_{c0} + \rho_{h0}$ decrease along the field line from the ionosphere to the equator. The cut-off frequency ω_*^2 monotonically rises equatorward, and if its value at the equator exceeds ω^2, the opaque region around the equator can appear, where $\omega^2 < \omega_*^2$.

For field lines intersecting the plasma sheet, the density after a monotonic fall increases considerably in the plasma sheet region. As a result, it is possible for a transparent region near the magnetospheric equatorial plane (top of a field line) between two opaque regions to appear. In this case, however, the transparent region at the top of a field line seems to be too narrow to provide a resonator for coupled Alfvén and SMS waves. Near the cut-off frequency the Alfvénic branch wavelength is very large, so the occurrence of a finite-scale non-transparent region cannot prevent the tunneling of Alfvénic mode through this region.

4. Dispersion curves for two-component plasma

The dispersion equation for the two-component plasma besides the parameters ρ_0, T, B_0, κ_P, κ_c, and $\sin^2\theta$, holds the new parameter μ. The dependence of dimensionless frequency $\Omega_\pm = \omega_\pm(\kappa_c V_A \sin\theta)^{-1}$ on dimensionless wave number $\kappa_\parallel = k_\parallel(\kappa_c \sin\theta)^{-1}$ for a set of the new parameter μ values is given in Figs. 1–4. For the taken normalization of frequency and wave number, the asymptotics of the Alfvénic branch have a unit slope, whereas the slope of the magnetosonic branch asymptotics is V_{ms}^2/V_A^2. The total density $\rho_0 = \rho_{c0} + \rho_{h0}$, as well as V_A, is supposed to be fixed.

The influence of the hot component on plasma properties may be considered from two viewpoints:

(A) the parameter β is proportional to μ, while the temperature of the hot component is assumed to be constant; and

(B) the parameter β is fixed ($\beta = 1$ for the examples presented in figures), that is the hot component temperature is inversely proportional to μ.

For the case A, the dispersion curves are shown in Figs 1 (stable plasma $\kappa_P/\kappa_c < 0$) and 2 ($\kappa_P/\kappa_c > 0$, when plasma instability is possible). We consider the case when the temperature of the hot component is sufficiently high, so V_s^2 exceeds V_A^2 10 times. In this case the critical value of μ, when the Alfvénic and magnetosonic branches swap the asymptotics, is $\mu_T^* = 1 - V_A^2/V_s^2 = 0.9$. Thus, the range of μ values, when $V_A > V_{ms}$, is rather narrow. For $\mu < 0.9$ the magnetosonic branch is a fast one, whereas the Alfvénic branch is a slow one. The velocity of the magnetosonic branch increases rapidly with the decrease of the hot component fraction $\mu \to 0$: $V_{ms}/V_A = (0.1+\mu)^{-1/2} \sim \mu^{-1/2}$, until $\mu > 0.1$, up to the limiting velocity $V_s = \sqrt{10}V_A$. This behavior indicates that the fast wave propagation involves the hot component only, which explains the increase of $V_{ms} \propto \rho_{0h}^{-1/2}$ upon the decrease of hot component density ρ_{0h}.

The interval of unstable $k_\parallel$ (Fig. 2) evidently shrinks upon the decrease of μ, and consequently β, according to the condition (3.4). In a two-component plasma only the slow branch $\omega_-(k_\parallel)$ can be unstable, whereas the fast branch $\omega_+(k_\parallel)$ is always stable. In the case of the one-component plasma ($\mu = 1$), this conclusion means

https://doi.org/10.1017/S0022377813001347 Published online by Cambridge University Press

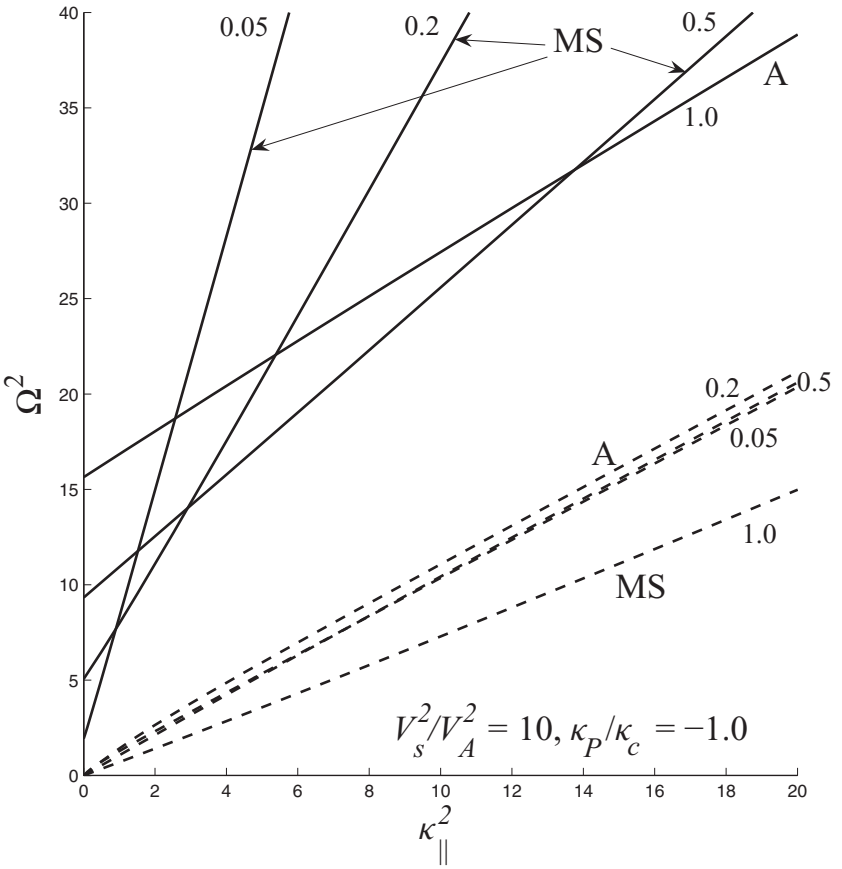


FIGURE 1. The dispersion curves $\omega_+(k_\parallel)$ (solid lines) and $\omega_-(k_\parallel)$ (dashed lines) in the plane of squared dimensionless parameters $\Omega = \omega/(\kappa_c V_A \sin\theta)$ and $\kappa_\parallel = k_\parallel/(\kappa_c \sin\theta)$ for various μ (indicated near curves) in the case $\kappa_P/\kappa_c = -1$ under fixed hot component temperature. The Alfvén branches are marked with A, and the magnetosonic branches — with MS.

the stability of Alfvénic mode and possible instability of the magnetosonic mode (Mazur et al. 2012). However, in a two-component plasma under a sufficiently small μ the association of fast and slow branches with Alvénic and magnetosonic modes (identified according to their short-wave asymptotics) changes. For the example given in Fig. 2, it is Alvénic mode that turns into slow branch at $\mu < 0.9$ and may become unstable. Notice that the polarization of an unstable mode does not correspond to either pure compressional or transverse disturbances, because $|b_3/b_1| \gtrsim 1/2$.

For case B, the dispersion curves are shown in Figs. 3 and 4. As in case A, the dispersion curves for Alfvénic and magnetosonic modes swap their asymptotics upon the decrease of μ below the critical value $\mu_\beta^* = \gamma\beta(2+\gamma\beta)^{-1}$ (for Figs. 3 and 4 $\mu_\beta^* = 5/11 \approx 0.45$). In contrast to case A, under fixed β the asymptotic velocity of the fast branch $V_{ms}^2/V_A^2 = \mu^{-1}\gamma\beta(2+\gamma\beta)^{-1}$ increases to infinity, because the hot component temperature $\propto \mu^{-1}$. Moreover, under fixed β the instability threshold and cut-off frequency do not depend on μ, as they are determined by parameter β according to (3.4) and (3.11), which do not hold parameter μ.

https://doi.org/10.1017/S0022377813001347 Published online by Cambridge University Press

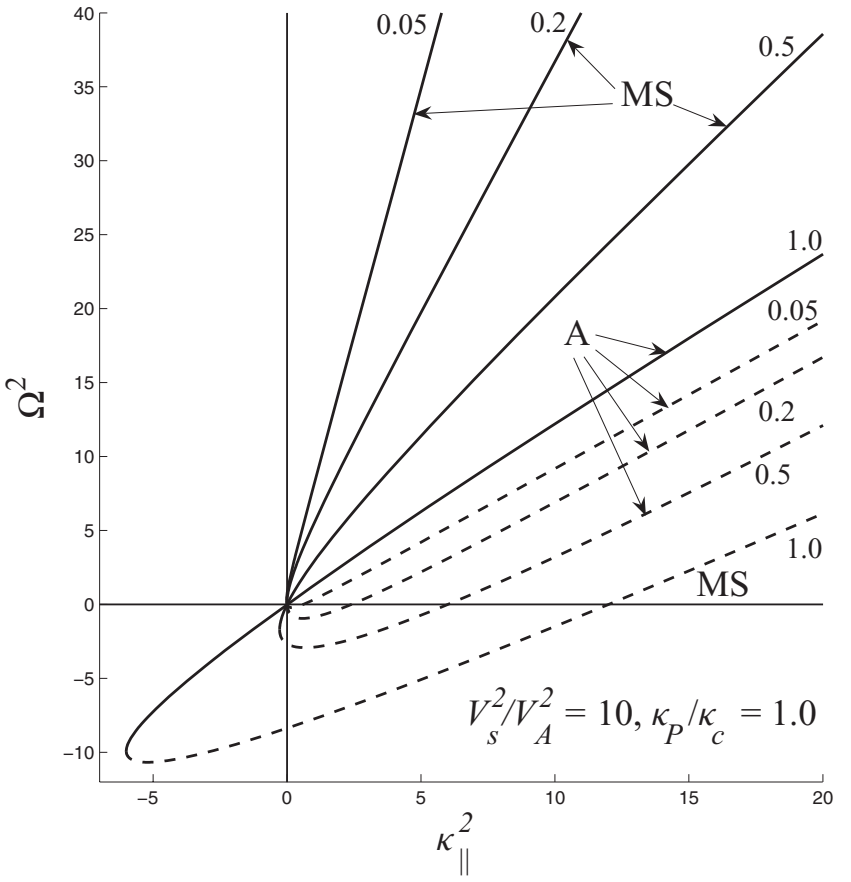


FIGURE 2. The same as in Fig. 1, but in the case $\kappa_P/\kappa_c = 1$, when plasma instability is possible.

4.1. *The growth rate of unstable disturbances*

The fastest growth rate of unstable disturbances at linear phase ($\propto \exp(\Gamma t)$) is determined by the minimum of $\Omega_-^2(\kappa_\parallel)$. From the expression for ω_-^2 (3.3) one can find that $\min \Omega_-^2 = -(1/4)\mu^{-1}\Lambda^2\beta^2(1+\lambda)^{-2}$, where $\Lambda = \kappa_P/\kappa_c$, $\lambda = [1-\tau\Lambda(2\gamma)^{-1}]^{1/2}$, and $\tau = (2+\gamma\beta-\gamma\beta\mu^{-1})/2$, is reached at

$$\kappa_\parallel^2 = \frac{\Lambda\beta}{1+\lambda}\left[1-\frac{(2+\gamma\beta)\Lambda}{4\gamma(1+\lambda)}\right].$$

Thus, the maximal growth rate

$$\max\Gamma = \frac{1}{2}\mu^{-1/2}(1+\lambda)^{-1}\beta\kappa_P V_A \sin\theta.$$

The comparison of $\min\Omega_-^2$ in one-component plasma ($\mu = 1$) and in two-component plasma with small addition of hot component $\mu \ll 1$ under the same β gives the ratio

$$\frac{\min\Omega_-^2(\mu \ll 1)}{\min\Omega_-^2(\mu = 1)} = \frac{4}{\Lambda\beta}(1+\sqrt{1-\Lambda/(2\gamma)})^2.$$

https://doi.org/10.1017/S0022377813001347 Published online by Cambridge University Press

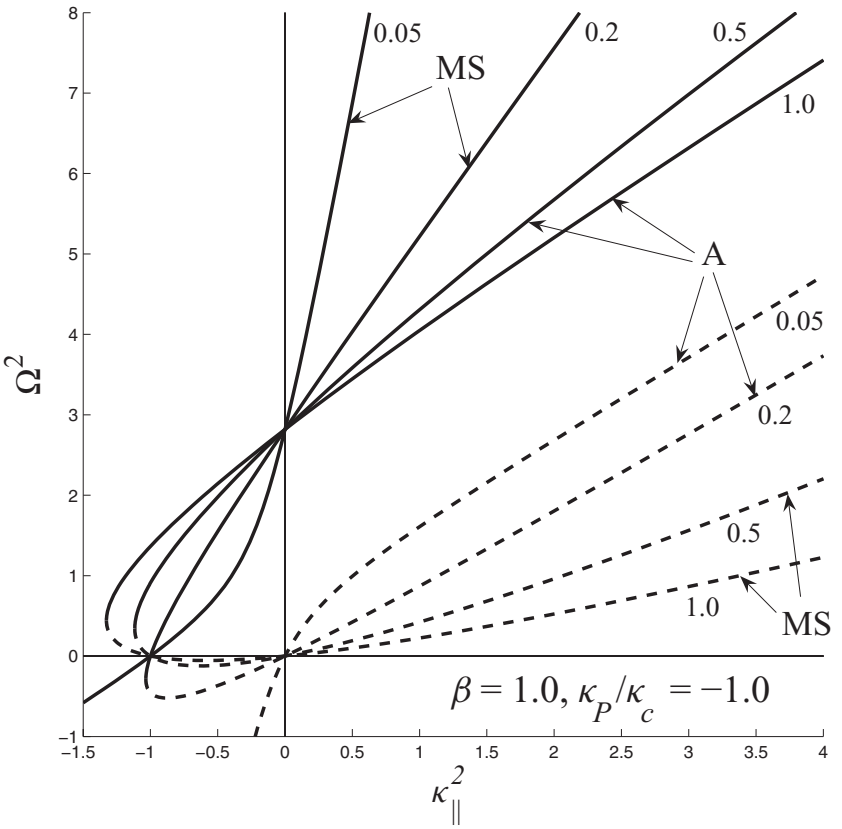


FIGURE 3. The same as in Fig. 1, but under fixed $\beta = 1$.

For the parameters $\Lambda = \beta = 1$, used in Fig. 4, this ratio is 13.5; therefore, the growth rate in the two-component is 3.7 times larger than in the one-component plasma.

5. Discussion

Analysis of the exact dispersion relationship (3.1) in the poloidal limit $k_1 = 0$ shows that the fast branch ω_+^2 is stable for any $k_\parallel^2$, that is, $\omega_+^2 \geqslant 0$. So, the conclusion about a possible instability of the fast mode, which in the case of one-component plasma corresponds to Alfvén mode (e.g. Miura et al. 1989; Ohtani and Tamao 1993), cannot be accepted.

Under favorable conditions for the ballooning instability on field lines, strongly extended into the magnetotail, the disturbance grows exponentially, though drift effects may produce oscillatory growth and azimuthal drift with the velocity about the Larmor drift velocity (Miura et al. 1989). The characteristic growth time of the instability, $\tau \simeq \Gamma^{-1} \simeq 30$ s, is about the typical time scale of the substorm explosive phase. When a system is near the threshold predicted by a linear instability theory, an external trigger may transfer a system into the state of nonlinear ('detonation') instability with an explosive growth (Hurricane et al. 1999).

However, an estimation of the instability criterion in the WKB approximation for a particular magnetic shell has an ultimately qualitative character. In a realistic magnetosphere, the ballooning modes are to be localized near the top of the field

https://doi.org/10.1017/S0022377813001347 Published online by Cambridge University Press

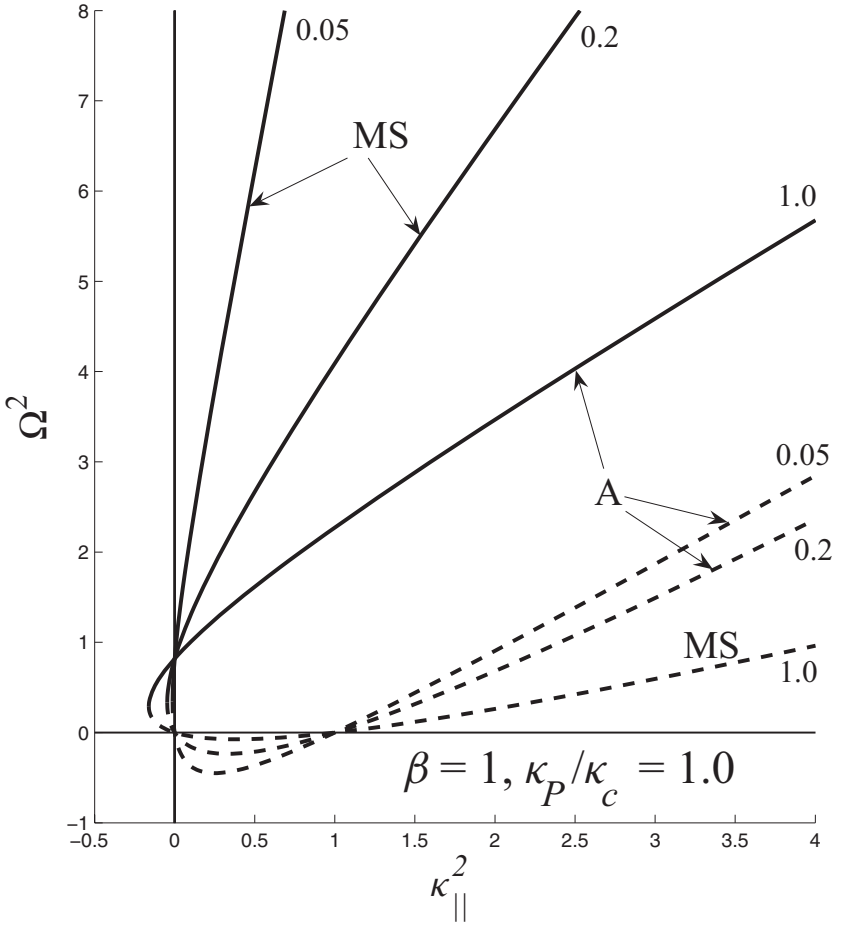


FIGURE 4. The same as in Fig. 3, but in the case $\kappa_P/\kappa_c = 1$, when plasma instability is possible.

line (in vicinity of the magnetospheric equatorial plane), where the β and curvature rapidly increase. However, $k_\parallel \to \infty$ in fact corresponds to the homogeneous case, and in this case the instability is absent according to (3.4).

The typical time scale of the substorm explosive phase (∼1–2 min) is much less than the Alfvén transit time along the extended field lines from the magnetotail to the ionosphere (∼10 min). Therefore, the influence of the ionospheric boundaries on the ballooning mode properties can be neglected, assuming that the growing disturbances are localized in the near-equatorial region of the nightside magnetosphere. The influence of the ionospheric boundary conditions on the ballooning modes was considered in many papers (e.g. Cheremnykh and Parnowski 2006). The imposing of boundary conditions at conjugate ionosphere results in quantization of $k_\parallel$ and occurrence of its imaginary components.

For the considered model the source of the free energy for the ballooning instability is the excess of the hot plasma pressure in the radial direction. However, this 2D model does not take into account certain factors that might be significant for the instability development: pressure anisotropy (Cheng and Qian 1994), drift effect (Pokhotelov et al. 1980; Klimushkin et al. 2012), kinetic effects (Klimushkin and Mager 2008), and

https://doi.org/10.1017/S0022377813001347 Published online by Cambridge University Press

the azimuthal pressure gradient related to a background field-aligned current (Ivanov et al. 1992; Golovchanskaya and Mingalev 2006).

Here we have considered coupled modes with MHD spatial scales. However, the ballooning modes with smaller time-space scales, which are to be modeled with kinetic approach, are possible. Thus, the instability with transverse scale of about ion Larmor radius can develop and form finger-like structure as three-dimensional particle-in-cell simulation showed (Pritchett and Coroniti 2010). The unstable mode was shown to be the low-frequency extension of the lower hybrid drift instability in straight magnetic geometry. The interchange-generated flow can intrude the near-Earth plasma sheet (Pritchett and Coroniti 2011). The satellite THEMIS observations indeed evidenced the feasibility of this kinetic ballooning/interchange in the terrestrial magnetotail (Panov et al. 2012).

6. Conclusion

The principal new feature of the two-component plasma is the possibility for a sound wave to propagate via the hot component only, whereas Alfvénic oscillations involve all plasma particles. This feature changes the dispersion curves for Alfvénic and SMS modes drastically, especially when the hot component fraction is small, and violates the correspondence between fast/slow branches and Alfvénic/magnetosonic modes.

In the region with a steep drop of the plasma pressure, held by curved magnetic field lines, an instability of the slow mode may become feasible. For fast waves with frequencies less than the cut-off frequency a non-transparent region may occur, which can influence the wave propagation along a field line.

Acknowledgements

The reported study was supported by RFBR grants 12-02-00031 (DK) and 13-05-90436 (EF), Program 22 of former Russian Academy of Sciences (NM), and grant ISSI 'MHD Oscillations in the Solar Corona and Earths Magnetosphere: Towards Consolidated Understanding' (VP). We appreciate constructive comments of the referee.

REFERENCES

Agapitov, A. V., Cheremnykh, O. K. and Parnowski, A. S. 2007 Ballooning perturbations in the inner magnetosphere of the Earth: spectrum, stability and eigenmode analysis. *Adv. Space Res.* **41**, 1682.

Cheng, C. Z. 2003 MHD field line resonances and global modes in three-dimensional magnetic fields. *J. Geophys. Res.* **108**(A1), 1002.

Cheng, C. Z. and Lin, C. S. 1987 Eigenmode analysis of compressional waves in the magnetosphere. *Geophys. Res. Lett.* **14**, 884.

Cheng, C. Z. and Qian, Q. 1994 Theory of ballooning-mirror instabilities for anisotropic pressure plasmas in the magnetosphere. *Geophys. Res. Lett.* **99**, 11193.

Cheng, C. Z., Qian, Q., Takahashi, K. and Lui, A. T. Y. 1994 Ballooning-mirror instability and internally driven Pc 4-5 wave events. *J. Geomagn. Geoelectr.* **46**, 997.

Cheremnykh, O. K. and Parnowski, A. S. 2004 The theory of ballooning perturbations in the inner magnetosphere of the Earth. *Adv. Space Res.* **33**, 769–773.

Cheremnykh, O. K. and Parnowski, A. S. 2006 Influence of ionospheric conductivity on the ballooning modes in the inner magnetosphere of the Earth. *Adv. Space Res.* **37**, 599–603.

https://doi.org/10.1017/S0022377813001347 Published online by Cambridge University Press

Du, J., Zhang, T. L., Nakamura, R., Wang, C., Baumjohann, W., Du, A. M., Volwerk, M., Glassmeier, K.-H. and McFadden, J. P. 2011 Mode conversion between Alfvén and slow waves observed in the magnetotail by THEMIS. *Geophys. Res. Lett.* **38**, L07101.

Golovchanskaya, I. V. and Maltsev, Y. P. 2005 On the identification of plasma sheet flapping waves observed by Cluster. *Geophys. Res. Lett.* **32**, L02102.

Golovchanskaya, I. V. and Mingalev, O. V. 2006 Propagation of the ballooning waves in the Earth's magnetotail. In: *Proc. 29th Ann. Sem. on 'Physics of Auroral Phenomena', Apatity, 27 February–3 March 2006*. Apatity: Kola Science Centre RAS, pp. 126–132.

Hurricane, O. A., Fong, B. H., Cowley, S. C., Coroniti, F. V., Kennel, C. F. and Pellat, R. 1999 Substorm detonation. *J. Geophys. Res.* **104**, 10221–10232.

Ivanov, V. N., Pokhotelov, O. A., Feygin, F. Z., Roux, A., Perrot, S. and Lekau, D. 1992 Balloon instability in the Earth's magnetosphere under non-constant pressure and finite β. *Geomagn. Aeronomy* **32**, 68–74.

Keiling, A. 2009 Alfvén waves and their roles in the dynamics of the Earth's magnetotail: a review. *Space Sci. Rev.* **142**, 73–156.

Klimushkin, D. Yu. 1998 Theory of azimuthally small-scale hydromagnetic waves in the axisymmetric magnetosphere with finite plasma pressure. *Ann. Geophys.* **16**, 303–321.

Klimushkin, D. Yu. and Mager, P. N. 2008 On the spatial structure and dispersion of slow magnetosonic modes coupled with Alfvén modes in planetary magnetospheres due to field line curvature. *Planet. Space Sci.* **56**, 1273.

Klimushkin, D. Yu., Mager, P. N. and Pilipenko, V. A. 2012 On the ballooning instability of the coupled Alfvén and drift compressional modes. *Earth Planets Space* **64**, 777–781.

Liu, W. W. 1997 Physics of the explosive growth phase: ballooning instability revisited. *J. Geophys. Res.* **102**, 4927–4931.

Mager, P. N., Klimushkin, D. Yu., Pilipenko, V. A. and Schafer, S. 2009 Field-aligned structure of poloidal Alfvén waves in a finite pressure plasma. *Ann. Geophys.* **27**, 3875–3882.

Mazur, N. G., Fedorov, E. N. and Pilipenko, V. A. 2012 Dispersion relation for ballooning modes and condition of their stability in near-Earth plasma. *Geomagn. Aeronomy* **52**, 603–612.

Miura, A., Ohtani, S. and Tamao, T. 1989 Ballooning instability and structure of diamagnetic waves in a model magnetosphere. *J. Geophys. Res.* **94**, 15231.

Nakamizo, A. and Iijima, T. 2003 A new perspective on magnetotail disturbances in terms of inherent diamagnetic processes. *J. Geophys. Res.* **108**, 1286.

Ohtani, S. and Tamao, T. 1993 Does the ballooning instability trigger substorms in the near-Earth magnetotail? *J. Geophys. Res.* **98**, 19369–19379.

Panov, E. V., Sergeev, V. A., Pritchett, P. L., Coroniti, F. V., Nakamura, R., Baumjohann, W., Angelopoulos, V., Auster, H. U. and McFadden, J. P. 2012 Observations of kinetic ballooning/interchange instability signatures in the magnetotail. *Geophys. Res. Lett.* **39**, L08110.

Pokhotelov, O. A., Buloshnikov, A. M. and Pilipenko, V. A. 1980 Hydromagnetic instability of the outer border of the trapped radiation. *Geomagn. Aeronomy* **20**, 419–424.

Pokhotelov, O. A., Pilipenko, V. A. and Amata, E. 1985 Drift-anisotropy instability of a finite-beta magnetospheric plasma. *Planet. Space Sci.* **33**(11), 1229–1241.

Pritchett, P. L. and Coroniti, F. V. 2010 A kinetic ballooning/interchange instability in the magnetotail. *J. Geophys. Res.* **115**, A06301.

Pritchett, P. L. and Coroniti F. V. 2011 Plasma sheet disruption by interchange-generated flow intrusions. *Geophys. Res. Lett.* **38**, L10102.

Raeder, J., Zhu, P., Ge, Y. and Siscoe, G. 2010 Open Geospace General Circulation Model simulation of a substorm: axial tail instability and ballooning mode preceding substorm onset. *J. Geophys. Res.* **115**, A00I16.

Roux, A., Perraut, S., Robert, P., Morane, A., Pedersen, A., Korth, A., Kremser, G., Aparicio, B., Rodgers, D. and Pellinen, R. 1991 Plasma sheet instability related to the westward travelling surge. *J. Geophys. Res.* **96**, 17697–17714.

Safargaleev, V. V. and Maltsev, Yu. P. 1986 Internal gravity waves in the plasmasheet. *Geomagn. Aeronomy* **26**, 220–223.

Southwood, D. J. and Saunders, M. A. 1985 Curvature coupling of slow and Alfvén MHD waves in a magnetotail field configuration. *Planet. Space Sci.* **33**, 127–134.

https://doi.org/10.1017/S0022377813001347 Published online by Cambridge University Press

Tsap, Y. T., Kopylova, Y. G., Stepanov, A. V., Melnikov, V. F. and Shibasaki, K. 2008 Ballooning instability in coronal flare loops. *Solar Phys.* **253**, 161–172.

Walker, A. D. M. 1987 Theory of magnetospheric standing hydromagnetic waves with large azimuthal wave number 1. Coupled Magnetosonic and Alfvén waves. *J. Geophys. Res.* **92**, 10039–10045.

Zhu, P., Raeder, J., Germaschewski, K. and Hegna, C. C. 2009 Initiation of ballooning instability in the near-Earth plasma sheet prior to the 23 March 2007 THEMIS substorm expansion onset. *Ann. Geophys.* **27**, 1129–1138.

https://doi.org/10.1017/S0022377813001347 Published online by Cambridge University Press